J. Fluid Mech. (1974), *vol.* 64, *part* 1, *pp.* 33–49
Printed in Great Britain

On the propulsion of micro-organisms near solid boundaries

By DAVID F. KATZ
Department of Applied Mathematics and Theoretical Physics, University of Cambridge

(Received 24 October 1973)

In this paper an infinite waving sheet is used to model a micro-organism swimming either parallel to a single plane wall, or along a channel formed by two such walls. The sheet surface, which undergoes small amplitude waves, can represent either a single flagellum or the envelope of the tips of numerous cilia. Two different solutions of the equations of motion are presented, depending upon whether or not the wave amplitude is small compared with the separation distances between the sheet and walls. It is found that the velocity of propulsion is bounded by the velocity of wave propagation by the sheet. Both the propulsive velocity and rate of working by the sheet increase as the separation distances decrease. However, it is demonstrated that suitable alterations in wave speed or wave shape can fix the rate of working while still causing increases in propulsive velocity. Reductions in propagated wave speed, i.e. beat frequency, are particularly effective in this regard.

1. Introduction

In recent years, the self-propulsion of micro-organisms has received increasing attention. Virtually all such studies to date have considered a single organism swimming in an otherwise undisturbed fluid of infinite extent. However, of great practical interest to the cell biologist, and obstetrician and gynaecologist, are situations in which micro-organisms are not physically isolated. During microscopic examination, the presence of a coverslip often constrains them to swim in a thin lamina of fluid of thickness the order of an organism length. Indeed, it has been speculated that this proximity to the coverslip may be responsible for the apparent discrepancy between existing hydrodynamic theories of self-propulsion and photographic data. Micro-organisms may be closely bunched together in suspension. Moreover, there exist instances, e.g. the case of spermatozoa *in vivo*, in which they are required to swim in close proximity to solid boundaries, possibly even narrow channel-like passages. It is, therefore, of great physical and physiological interest to consider the influence of nearby solid boundaries on self-propulsion at very low Reynolds number.

Taylor (1951) used a two-dimensional waving sheet in his pioneering study of the locomotion of an organism possessing a single flagellum, e.g. a spermatozoon and many protozoa. Blake (1971) also used a sheet as an envelope model for the propulsive effect of beating, tightly bunched cilia on the surface of a micro-

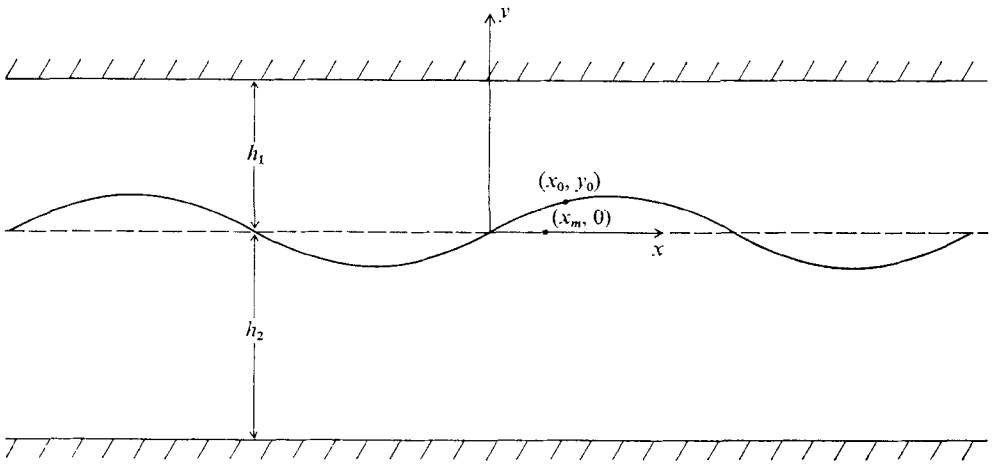

FIGURE 1. Waving sheet in channel. The wave velocity propagated *by the sheet* is $-c\mathbf{e}_x$. Viewed in a fixed frame of reference, the wave crests appear to translate with velocity $(V-c)\,\mathbf{e}_x$.

organism. Both these studies considered only isolated sheets. Reynolds (1965) used Taylor's sheet and approach to consider the effect of a rigid flat wall adjacent to the sheet. These analyses all make use of the assumption of small amplitude waves to apply boundary conditions expanded about the mean planes of the wavy sheets. Thus, a limitation on Reynolds' results is the requirement that the wave amplitude be small compared with the mean separation distances between the wavy sheet and the adjacent flat walls, both above and below it. The cases of self-propulsion in close proximity to a single wall, or in a narrow two-dimensional channel, are therefore excluded.

This paper considers a general wavy sheet swimming between two flat walls, cf. figure 1. Use of an infinite two-dimensional sheet to simulate the movements of a three-dimensional organism of finite length and width is, of course, a considerable simplification, which underestimates the spatial rate of decay of the hydrodynamic effects of an organism's motion. For a real organism swimming in a real three-dimensional fluid this rate of decay is greater than if the organism's effects on the fluid are constrained artificially to decay in two dimensions only. The two-dimensional model effectively treats the *parallel* swimming at a given distance from a wall of a very large number of organisms whose motions, being in phase, can reinforce one another: a problem with a certain biophysical interest in its own right. The model is put forward here, however, with the principal aim of indicating possible qualitative trends that may be applicable even to the motion of a single organism.

Other simplifications are that only periodic wave forms can be considered and that end effects, such as the presence of an inert head, are excluded. Indeed, both the swimming velocity and rate of working of a micro-organism depend upon its finite size. Nevertheless, this model is useful in suggesting the qualitative nature of wall effects upon propulsion of a micro-organism. We shall be interested here in the extent to which the wall separation distances influence the

swimming velocity and rate of working, and how variations in the wave shape and propagated wave speed alter these influences. Detailed information, regarding swimming trajectories, for example, is beyond the scope of this approach.

Use of the wavy-sheet model requires that the fluid equations of motion be solved in the regions above and below the sheet. When the mean separation distances between the sheet and the two walls are of equal magnitude, the 'upper' and 'lower' problems are, thus, similar. If, however, one of the walls is relatively close to the sheet and the other is not, then different problems must be posed, solved and combined for the upper and lower regions. We shall examine all such possibilities here.

We consider a sheet propagating a transverse wave in the negative-x direction with wave speed c. This gives rise to a translation of all points on the sheet with 'propulsive' velocity V in the positive-x direction. Viewed in a co-ordinate frame fixed in space, the apparent wave speed of the sheet is thus $(V-c)\,\mathbf{e}_x$. Letting (x_0, y_0) be a point on the sheet surface, as seen in the fixed frame, we consider

$$\left.\begin{aligned} x_0 &= x_m + a\cos k[x_m + (c-V)\,t] + d\sin k\,[x_m + (c-V)\,t], \\ y_0 &= b\sin k[x_m + (c-V)\,t]. \end{aligned}\right\} \tag{1}$$

In this 'Lagrangian' representation of the sheet surface $(x_m, 0)$ is the mean position of (x_0, y_0). The path of (x_0, y_0), seen in a frame translating with velocity $V\mathbf{e}_x$, is an ellipse inclined to the x axis at angle $\frac{1}{2}\tan^{-1}[4bd/(a^2+d^2-b^2)]$. Although this surface representation is different from Taylor's, his lowest-order results, which are of interest here, are obtained for the case $a = d = 0$. Non-zero d and a enable us to model a slightly more general flagellar beat, or the ciliary symplectic metachronal wave discussed by Blake. Clearly $u(x_0, y_0) = dx_0/dt$ and $v(x_0, y_0) = dy_0/dt$. It will prove convenient to work in a co-ordinate frame in which the crests of the waves on the sheet do not appear to translate. Hence we introduce $z \equiv x + (c-V)\,t$ and have, in the z frame,

$$z_0 = z_m + a\cos kz_m + d\sin kz_m, \quad y_0 = b\sin kz_m. \tag{2}$$

Thence,

$$\left.\begin{aligned} u(z_0, y_0) &= c - V + c[-ak\sin kz_m + dk\cos kz_m], \\ v(z_0, y_0) &= c(bk)\cos kz_m. \end{aligned}\right\} \tag{3}$$

The unit outer normal $\mathbf{n}$ to the sheet is given by

$$\mathbf{n} = \mathbf{e}_z[\mp bk\cos kz_m + O(bk)^3] + \mathbf{e}_y[\pm 1 + O(bk)^2], \tag{4}$$

where the upper and lower signs refer to the upper and lower surfaces of the sheet, respectively. The local stress $\boldsymbol{\sigma}$ exerted by the fluid on the sheet is then

$$\begin{aligned} \boldsymbol{\sigma} = \mathbf{e}_z &\left[\left(-p + 2\mu\frac{\partial u}{\partial y}\right)(\mp bk\cos kz_m + \ldots) + \mu\left(\frac{\partial u}{\partial y} + \frac{\partial v}{\partial z}\right)(\pm 1 + \ldots)\right]_{(z_0,\, y_0)} \\ &+ \mathbf{e}_y\left[\mu\left(\frac{\partial u}{\partial y} + \frac{\partial v}{\partial z}\right)(\mp bk\cos kz_m + \ldots) + \left(-p + 2\mu\frac{\partial v}{\partial y}\right)(\pm 1 + \ldots)\right]_{(z_0,\, y_0)} \end{aligned} \tag{5}$$

Characteristic of a wavy sheet swimming between walls is the general inability of the boundary conditions on velocity completely to determine the motion.

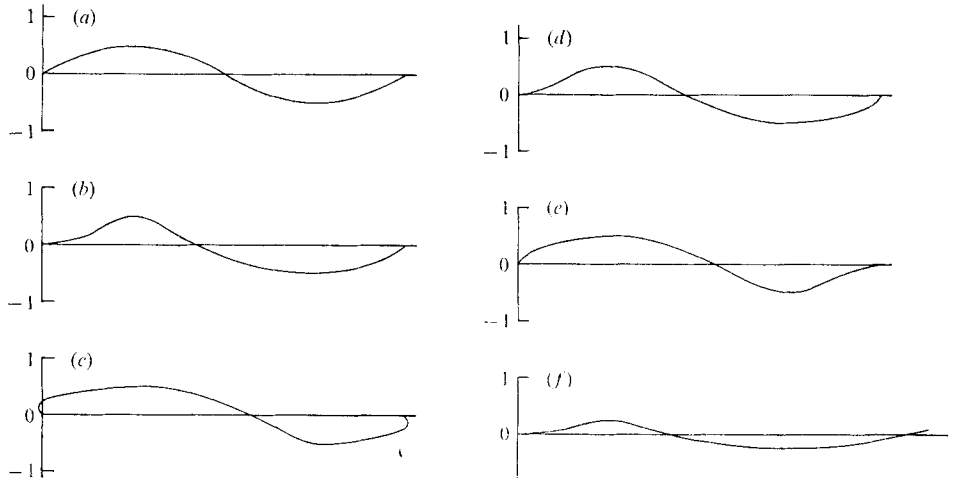

FIGURE 2. Some examples of wavy-sheet shapes, all with $d = 0$. (*a*) $ka = 0$, $kb = 0{\cdot}5$. (*b*) $ka = 0{\cdot}5$, $kb = 0{\cdot}5$. (*c*) $ka = -0{\cdot}5$, $kb = 0{\cdot}5$. (*d*) $ka = 0{\cdot}25$, $kb = 0{\cdot}5$. (*e*) $ka = -0{\cdot}25$, $kb = 0{\cdot}5$, (*f*) $ka = 0{\cdot}5$, $kb = 0{\cdot}25$.

Dynamical considerations, in addition to kinematical ones, must be invoked. The net pressure difference between upstream and downstream infinity must be specified. We shall assume here that this difference is zero. Since the sheet will be swimming at constant velocity, we expect the average force on the sheet per wavelength (and unit depth) to vanish. This force $\mathscr{F}$ is the sum of contributions from the upper and lower sheet surfaces:

$$\mathscr{F} = \langle \boldsymbol{\sigma} \rangle_u + \langle \boldsymbol{\sigma} \rangle_l = 0, \tag{6}$$

where angular brackets indicate an average over a wavelength. The average stress $\boldsymbol{\sigma}_w$ per sheet wavelength exerted by the fluid on the walls is

$$\boldsymbol{\sigma}_w = \mp \mu \left\langle \left(\frac{\partial u}{\partial y} + \frac{\partial v}{\partial z} \right)_{y=h_1,\, -h_2} \right\rangle \mathbf{e}_z \pm \langle p_{y=h_1,\, -h2} \rangle \, \mathbf{e}_y. \tag{7}$$

Since the Reynolds number is small, and there is no externally applied pressure gradient, the momentum theorem requires

$$\langle \boldsymbol{\sigma} \rangle_{u,l} + \langle \boldsymbol{\sigma}_w \rangle_{u,l} = 0. \tag{8}$$

If M is the local moment on the sheet due to fluid reactions above and below it,

$$\begin{aligned} M(z_0, y_0) &= M(0, y_0) + \int_0^{z_0} [(z_0 - z_0') \, \Delta\sigma_y(z_0', y_0') - (y_0 - y_0') \, \Delta\sigma_z(z_0', y_0')] \, ds \\ &\doteqdot M(0, y_0) + \int_0^{z_0} (z_0 - z_0') \, \Delta\sigma_y(z_0', y_0') \, dz_0' + \ldots, \end{aligned} \tag{9}$$

where $\Delta\sigma_z$ and $\Delta\sigma_y$ are the z and y components of $\Delta\boldsymbol{\sigma} \equiv \boldsymbol{\sigma}_u + \boldsymbol{\sigma}_l$, and ds is the element of sheet arc length. Moment equilibrium of the sheet requires

$$\langle M \rangle = 0. \tag{10}$$

We shall have recourse to all these conditions in the subsequent development. Finally E, the average rate of working per wavelength by the sheet on the fluid, is the sum of contributions from the upper and lower surfaces:

$$E = \langle (\mathbf{u} \,.\, \Delta\boldsymbol{\sigma})_{(z_0, y_0)} \rangle. \tag{11}$$

2. Biharmonic analysis

Consider now the case $h_1 k \geqslant O(1)$, $h_2 k \geqslant O(1)$, thus $b \ll h_1, h_2$. An appropriate length scale here for changes in both the z and y directions is the wavelength $2\pi/k$, and we introduce the following dimensionless variables:

$$\left.\begin{gathered} \tilde{z} \equiv kz, \quad \tilde{y} \equiv ky, \quad \tilde{\psi} \equiv k\psi/c, \\ \tilde{u} \equiv u/c, \quad \tilde{v} \equiv v/c, \quad \tilde{p} \equiv (p - p_\infty)/\mu c k, \\ \epsilon\tilde{a} \equiv ka, \quad \epsilon\tilde{b} \equiv kb, \quad \epsilon\tilde{d} \equiv kd; \\ \epsilon \ll 1, \quad \tilde{b} = O(1), \quad \tilde{a} \leqslant O(1), \quad \tilde{d} \leqslant O(1). \end{gathered}\right\}$$

Here ψ is the stream function and p the pressure, p_∞ being the pressure at $z = \pm\infty$. For the very small Reynolds number of interest, the following problem results:

$$\left.\begin{gathered} \tilde{\nabla}^4 \tilde{\psi} = 0, \quad \tilde{u} = \partial\tilde{\psi}/\partial\tilde{y}, \quad \tilde{v} = -\partial\tilde{\psi}/\partial\tilde{z}, \\ \partial\tilde{p}/\partial\tilde{z} = \partial(\tilde{\nabla}^2\tilde{\psi})/\partial\tilde{y}, \quad \partial\tilde{p}/\partial\tilde{y} = -\partial(\tilde{\nabla}^2\tilde{\psi})/\partial\tilde{z}, \end{gathered}\right\} \tag{12}$$

$$\left.\begin{gathered} \tilde{y}_0 = \epsilon\tilde{b}\sin\tilde{z}_m, \quad \tilde{z}_0 = \tilde{z}_m + \epsilon(\tilde{a}\cos\tilde{z}_m + \tilde{d}\sin\tilde{z}_m), \\ \tilde{u}(\tilde{z}_0, \tilde{y}_0) = 1 - \tilde{V} + \epsilon(-\tilde{a}\sin\tilde{z}_m + \tilde{d}\cos\tilde{z}_m), \quad \tilde{v}(\tilde{z}_0, \tilde{y}_0) = \epsilon\tilde{b}\cos\tilde{z}_m, \\ \tilde{u}(\tilde{z}, \tilde{h}_1) = \tilde{u}(\tilde{z}, -\tilde{h}_2) = \tilde{v}(\tilde{z}, \tilde{h}_1) = \tilde{v}(\tilde{z}, -\tilde{h}_2) = 0, \quad \tilde{p}(\pm\infty, \tilde{y}) = 0. \end{gathered}\right\} \tag{13}$$

Solution of this problem proceeds just as in the analyses by Taylor and Reynolds or, equivalently, by Blake. The dependent variables are expanded in ascending powers of the small parameter ϵ, and the boundary conditions at $(\tilde{z}_0, \tilde{y}_0)$ are expanded in Taylor series about the mean position $(\tilde{z}_m, 0)$. In each equation, the coefficient of ϵ^n is equated to zero for each n. A hierarchy of biharmonic problems results, with kinematic boundary conditions applied on the planes $\tilde{y} = 0$, $\tilde{y} = \tilde{h}_1$ and $\tilde{y} = -\tilde{h}_2$.

In the following development, we shall consider a separation distance $\tilde{h}$, equal to $\tilde{h}_1$ or $-\tilde{h}_2$, as necessary. Letting a subscript denote the power of ϵ of interest, we have at 'zero order'

$$\left.\begin{gathered} \tilde{\nabla}^4\tilde{\psi}_0 = 0, \\ \partial\tilde{\psi}_0(\tilde{z}, 0)/\partial\tilde{y} = 1 - \tilde{V}_0, \quad \partial\tilde{\psi}_0(\tilde{z}, 0)/\partial\tilde{z} = 0, \\ \partial\tilde{\psi}_0(\tilde{z}, \tilde{h})/\partial\tilde{y} = 1, \quad \partial\tilde{\psi}_0(\tilde{z}, \tilde{h})/\partial\tilde{z} = 0. \end{gathered}\right\} \tag{14}$$

Thus

$$\tilde{\psi}_0 = \tilde{y} + \tilde{V}_0(\tilde{y}^2/2\tilde{h} - \tilde{y}). \tag{15}$$

Since there are no externally applied forces acting here on the sheet or walls, we take $\tilde{V}_0 = 0$.

The 'first-order' problem is

$$\tilde{\nabla}^4\tilde{\psi}_1 = 0, \tag{16}$$

$$\partial\tilde{\psi}_1(\tilde{z}, 0)/\partial\tilde{y} = -\tilde{V}_1 - \tilde{a}\sin\tilde{z} + \tilde{d}\cos\tilde{z}, \tag{17}$$

$$\partial\tilde{\psi}_1(\tilde{z}, 0)/\partial\tilde{z} = -\tilde{b}\cos\tilde{z}, \tag{18}$$

$$\partial\tilde{\psi}_1(\tilde{z}, \tilde{h})/\partial\tilde{y} = \partial\tilde{\psi}_1(\tilde{z}, \tilde{h})/\partial\tilde{z} = 0. \tag{19), (20}$$

We obtain

$$\tilde{\psi}_1(\tilde{z},\tilde{y}) = [(\tilde{A}_1\tilde{y}+\tilde{B}_1)\sin\tilde{z}+(\tilde{C}_1\tilde{y}+\tilde{D}_1)\cos\tilde{z}]\sinh\tilde{y} + [(\tilde{E}_1\tilde{y}-1)\sin\tilde{z}+\tilde{G}_1\tilde{y}\cos\tilde{z}]\cosh\tilde{y}, \quad (21)$$

$$\tilde{p}_1(\tilde{z},\tilde{y}) = 2[(\tilde{C}_1\sin\tilde{z}-\tilde{A}_1\cos\tilde{z})\sinh\tilde{y}+(\tilde{G}_1\sin\tilde{z}-\tilde{E}_1\cos\tilde{z})\cosh\tilde{y}], \quad (22)$$

with

$$\tilde{A}_1 = \frac{\tilde{b}\sinh^2\tilde{h}+\tilde{a}[\sinh\tilde{h}\cosh\tilde{h}-\tilde{h}]}{\sinh^2\tilde{h}-\tilde{h}^2},$$

$$\tilde{B}_1 = -(\tilde{E}_1+\tilde{a}) = \frac{\tilde{b}[\sinh\tilde{h}\cosh\tilde{h}+\tilde{h}]+\tilde{a}\tilde{h}^2}{\sinh^2\tilde{h}-\tilde{h}^2},$$

$$\tilde{C}_1 = -\frac{\tilde{d}[\sinh\tilde{h}\cosh\tilde{h}-\tilde{h}]}{\sinh^2\tilde{h}-\tilde{h}^2},$$

$$\tilde{G}_1 = \tilde{d}-\tilde{D}_1 = \frac{\tilde{d}\sinh^2\tilde{h}}{\sinh^2\tilde{h}-\tilde{h}^2}.$$

We have taken $\tilde{V}_1 = 0$, just as previously; when the flows in both the upper and lower regions are biharmonic, i.e. $kh \geqslant O(1)$, then propulsion is of second order in ϵ.

Now to determine $\tilde{V}_2$, we need consider only the z-independent terms in the boundary conditions for $\tilde{u}_2$ at $\tilde{y} = 0$ and $\tilde{y} = \tilde{h}$. These are

$$\frac{\partial\tilde{\psi}_2}{\partial\tilde{y}}(\tilde{z},0) = -(\tilde{a}\cos\tilde{z}+\tilde{d}\sin\tilde{z})\frac{\partial^2\tilde{\psi}_1}{\partial\tilde{z}\,\partial\tilde{y}}(\tilde{z},0)-\tilde{b}\sin\tilde{z}\frac{\partial^2\tilde{\psi}_1}{\partial\tilde{y}^2}(\tilde{z},0)+\tilde{V}_2$$

$$= \tilde{V}_2+\tfrac{1}{2}\tilde{a}^2+\tilde{d}^2-\frac{\tilde{b}^2[\sinh^2\tilde{h}+\tilde{h}^2]+2\tilde{a}\tilde{b}[\sinh\tilde{h}\cosh\tilde{h}-\tilde{h}]}{\sinh^2\tilde{h}-\tilde{h}^2}+f_n(z), \quad (23)$$

$$\partial\tilde{\psi}_2(\tilde{z},\tilde{h})/\partial\tilde{y} = 0. \quad (24)$$

We can introduce an expression for $\tilde{\psi}_2$ analogous to equation (21) for $\tilde{\psi}_1$, but we must also include the eigensolutions $\tilde{\mathscr{A}}_2\tilde{y}+\tilde{\mathscr{B}}_2\tilde{y}^2$. Thence, from (23) and (24),

$$\tilde{V}_2 = \frac{1}{2}\left\{\tilde{b}^2\left[\frac{\sinh^2\tilde{h}+\tilde{h}^2}{\sinh^2\tilde{h}-\tilde{h}^2}\right]-(\tilde{a}^2+\tilde{d}^2)\right\}+\tilde{a}\tilde{b}\left[\frac{\sinh\tilde{h}\cosh\tilde{h}-\tilde{h}}{\sinh^2\tilde{h}-\tilde{h}^2}\right]-2\tilde{\mathscr{B}}_2\tilde{h}. \quad (25)$$

Note that $\tilde{\mathscr{B}}_2$ cannot be determined from the kinematics of the problem. Since we are generally interested in $\tilde{h}_1 \neq \tilde{h}_2$, we have two expressions for $\tilde{V}_2$, cf. (25), and thus two values of $\tilde{\mathscr{B}}_2$. Consider now the force equilibrium of the sheet, cf. (6). To lowest order,

$$\tilde{\mathscr{F}}\cdot\mathbf{e}_z = (\mu ck)\,2\epsilon^2(\tilde{\mathscr{B}}_{2u}-\tilde{\mathscr{B}}_{2l}) = 0. \quad (26)$$

Thus $\tilde{\mathscr{B}}_{2u} = \tilde{\mathscr{B}}_{2l} \equiv \tilde{\mathscr{B}}_2$. Thence, since the upper and lower solutions must yield the same value of $\tilde{V}_2$, we obtain

$$\tilde{\mathscr{B}}_2 = \frac{1}{2(\tilde{h}_1+\tilde{h}_2)}\left\{\frac{\tilde{b}^2}{2}\left[\frac{\sinh^2\tilde{h}_1+\tilde{h}_1^2}{\sinh^2\tilde{h}_1-\tilde{h}_1}-\frac{\sinh^2\tilde{h}_2+\tilde{h}_2^2}{\sinh^2\tilde{h}_2-\tilde{h}_2^2}\right]\right.$$
$$\left.+\tilde{a}\tilde{b}\left[\frac{\sinh\tilde{h}_1\cosh\tilde{h}_1-\tilde{h}_1}{\sinh^2\tilde{h}_1-\tilde{h}_1^2}-\frac{\sinh\tilde{h}_2\cosh\tilde{h}_2-\tilde{h}_2}{\sinh^2\tilde{h}_2-\tilde{h}_2^2}\right]\right\}, \quad (27)$$

$$\epsilon^2\tilde{V}_2 = \frac{\epsilon^2}{2(\tilde{h}_1+\tilde{h}_2)}\left\{\tilde{b}^2\left[\frac{\tilde{h}_2}{2}\frac{\sinh^2\tilde{h}_1+\tilde{h}_1^2}{\sinh^2\tilde{h}_1-\tilde{h}_1^2}+\frac{\tilde{h}_1}{2}\frac{\sinh^2\tilde{h}_2+\tilde{h}_2^2}{\sinh^2\tilde{h}_2-\tilde{h}_2^2}\right]\right.$$
$$\left.+\tilde{a}\tilde{b}\left[\tilde{h}_2\frac{\sinh\tilde{h}_1\cosh\tilde{h}_1-\tilde{h}_1}{\sinh^2\tilde{h}_1-\tilde{h}_1^2}+\tilde{h}_1\frac{\sinh\tilde{h}_2\cosh\tilde{h}_2-\tilde{h}_2}{\sinh^2\tilde{h}_2-\tilde{h}_2^2}\right]\right\}-\frac{\epsilon^2}{2}(\tilde{a}^2+\tilde{d}^2). \quad (28)$$

The average rate of working is to lowest order

$$E = (\mu c^2 k)\,\epsilon^2 \left\{ \frac{\tilde{b}^2[\sinh\tilde{h}_1\cosh\tilde{h}_1+\tilde{h}_1]+2\tilde{a}\tilde{b}\tilde{h}_1^2+(\tilde{a}^2+\tilde{d}^2)[\sinh\tilde{h}_1\cosh\tilde{h}-\tilde{h}_1]}{\sinh^2\tilde{h}_1-\tilde{h}_1^2} \right.$$
$$\left. + \frac{\tilde{b}^2[\sinh\tilde{h}_2\cosh\tilde{h}_2+\tilde{h}_2]+2\tilde{a}\tilde{b}\tilde{h}_2^2+(\tilde{a}^2+\tilde{d}^2)[\sinh\tilde{h}_2\cosh\tilde{h}_2-\tilde{h}_2]}{\sinh^2\tilde{h}_2-\tilde{h}_2^2} \right\}. \quad (29)$$

Regarding (27)–(29), several points are worth noting. The existence of a non-zero for finite $\tilde{h}_1 \neq \tilde{h}_2$ means that a $\tilde{\mathscr{B}}_2$ torque will tend to turn a sheet of finite thickness away from the near wall. The centre of the channel $\tilde{h}_1 = \tilde{h}_2$ is thus the 'preferred' position, at which $\tilde{\mathscr{B}}_2 = 0$, cf. (27). If, on the other hand, one wall is removed to infinity, say $\tilde{h}_2 \to -\infty$ with $\tilde{h}_1$ finite, then $\mathscr{B}_2 \to 0$ as $1/\tilde{h}_2$. In both these situations, then, the torque vanishes.

Note that the $\tilde{d}^2$ term in (28) is independent of $\tilde{h}$. The proximity of walls does not alter the effect of the particle path inclination on propulsion. Of course, as $\tilde{h}_1 \to |\tilde{h}_2| \to \infty$,

$$\epsilon^2\tilde{V}_2 \to \tfrac{1}{2}\epsilon^2(\tilde{b}^2+2\tilde{a}\tilde{b}-\tilde{a}^2-\tilde{d}^2), \quad (30)$$

$$\tfrac{1}{2}E/\mu c^2 k \to \epsilon^2(\tilde{b}^2+\tilde{a}^2+\tilde{d}^2), \quad (31)$$

the values obtained by Blake. Blake noted that transverse and longitudinal surface oscillations tend to propel an isolated sheet in opposite directions, antiparallel or parallel to the direction of the metachronal wave, respectively. From (28) we note that the presence of walls does not alter this tendency. However, the relative importance of transverse oscillations is amplified. For example, when $\tilde{d} = 0$, $\epsilon^2\tilde{V}_2 = \frac{1}{2}\epsilon^2(\tilde{b}+2\tilde{a}\tilde{b}-\tilde{a}^2)$ for the isolated sheet. Correspondingly, if $\tilde{h}_2 \to -\infty$ and $\tilde{h}_1 = 2$, then $\epsilon^2\tilde{V}_2 = \frac{1}{2}\epsilon^2(1{\cdot}87\tilde{b}^2+2{\cdot}54\tilde{a}\tilde{b}-\tilde{a}^2)$ for a non-isolated sheet. We shall defer a discussion of propulsive efficiency to §5.

3. Lubrication-theory analysis

We next examine the case $h_1 k \ll 1$, $h_2 k \ll 1$. Since the biharmonic analysis is valid only when $b \ll h_1, h_2$, the wave amplitude would have to be very small indeed! We wish to consider $b = O(h_1, h_2)$, the case of a sheet swimming in a narrow channel. Here an appropriate length scale for changes in the y direction is b (or h_1 or h_2) rather than $2\pi/k$. For purposes of comparison we shall choose b, and define the following dimensionless variables:

$$\hat{z} \equiv k\hat{z}, \quad \hat{y} \equiv y/b, \quad \hat{p} \equiv (p-p_\infty)\,b^2k/\mu c,$$
$$\hat{u} \equiv u/c, \quad \hat{v} \equiv v/(bk)\,c.$$

In these variables, the governing equations become

$$\left.\begin{aligned} (bk)^2\frac{\partial^2\hat{u}}{\partial\hat{z}^2}+\frac{\partial^2\hat{u}}{\partial\hat{y}^2} &= \frac{\partial\hat{p}}{\partial\hat{z}}, \\ (bk)^4\frac{\partial^2\hat{v}}{\partial\hat{z}^2}+(bk)^2\frac{\partial^2\hat{v}}{\partial\hat{y}^2} &= \frac{\partial\hat{p}}{\partial\hat{y}}, \\ \partial\hat{u}/\partial\hat{z}+\partial\hat{v}/\partial\hat{y} &= 0, \end{aligned}\right\} \quad (32)$$

with boundary conditions

$$\left.\begin{gathered}\hat{y}_0 = \epsilon\tilde{b}\sin\hat{z}_m, \quad \hat{z}_0 = \hat{z}_m + \epsilon(\tilde{a}\cos\hat{z}_m + \tilde{d}\sin\hat{z}_m), \\ \hat{u}(\hat{z}_0, \hat{y}_0) = 1 - \hat{V} + \epsilon(\tilde{d}\cos\hat{z}_m - \tilde{a}\sin\hat{z}_m), \quad \hat{v}(\hat{z}_0, \hat{y}_0) = \tilde{b}\cos\hat{z}_m, \\ \hat{u}(\hat{z}, \hat{h}) = 1, \quad \hat{v}(\hat{z}, \hat{h}) = 0, \\ \hat{h} = h_1/b \quad \text{or} \quad -h_2/b.\end{gathered}\right\} \tag{33}$$

An expansion in ϵ is again suggested. We obtain to lowest order

$$\partial^2\hat{u}_0/\partial\hat{y}^2 = \partial\hat{p}_0/\partial\hat{z}, \quad \partial\hat{p}_0/\partial\hat{y} = 0, \tag{34), (35}$$

$$\partial\hat{u}_0/\partial\hat{z} + \partial\hat{v}_0/\partial\hat{y} = 0, \tag{36}$$

$$\hat{u}_0(\hat{z}_0, \hat{y}_0) = 1 - \hat{V}_0, \quad \hat{v}_0(\hat{z}_0, \hat{y}_0) = \tilde{b}\cos\hat{z}_m, \tag{37), (38}$$

$$\hat{u}_0(\hat{z}, \hat{h}) = 1, \quad \hat{v}_0(\hat{z}, \hat{h}) = 0, \tag{39), (40}$$

$$\hat{p}_0(\pm\infty, \hat{y}) = 0. \tag{41}$$

Equations (34)–(36) are the familiar equations of lubrication theory. Note that the velocities due to z-wise stretching of the sheet are of higher order and do not appear. We obtain

$$\hat{u}_0 = \frac{1}{2}\frac{d\hat{p}_0}{d\hat{z}}[(\hat{y}+\hat{h})^2 - (\hat{h}+\sin\hat{z})(\hat{y}+\hat{h})] + \hat{V}_0\left(\frac{\hat{y}}{\hat{h}+\sin\hat{z}} - 1\right) + 1, \tag{42}$$

$$\hat{v}_0 = \frac{1}{2}\frac{d^2\hat{p}_0}{d\hat{z}^2}\left[\frac{(\hat{y}+\hat{h})^2}{2}(\hat{h}+\sin\hat{z}) - \frac{(\hat{y}+\hat{h})^3}{3}\right] + \frac{1}{4}\frac{d\hat{p}_0}{d\hat{z}}(\hat{y}+\hat{h})^2\cos\hat{z} + \tfrac{1}{2}\hat{V}_0\left[\frac{(\hat{y}+\hat{h})^2\cos\hat{z}}{(\hat{h}+\sin\hat{z})^2}\right]. \tag{43}$$

Here we have used the expansion

$$\frac{d\hat{p}_0}{d\hat{z}}(\hat{z}_0, 0) = \frac{d\hat{p}_0}{d\hat{z}}(\hat{z}_m, 0) + \epsilon(\tilde{a}\cos\hat{z}_m + \tilde{d}\sin\hat{z}_m)\frac{d^2\hat{p}_0}{d\hat{z}^2}(\hat{z}_m, 0) + \ldots,$$

retaining only the first term since we are working to lowest order. Equations (38) and (43) then yield a 'Reynolds equation' for pressure:

$$\frac{d}{d\hat{z}}\left(\frac{d\hat{p}_0}{d\hat{z}}\right) + 3\left(\frac{d\hat{p}_0}{d\hat{z}}\right)\frac{\cos\hat{z}}{\hat{h}+\sin\hat{z}} = -\frac{(12+6\hat{V}_0)\cos\hat{z}}{(\hat{h}+\sin\hat{z})^3}. \tag{44}$$

Integrating yields

$$\frac{d\hat{p}_0}{d\hat{z}} = \frac{\hat{A}_0 - (12+6\hat{V}_0)\sin\hat{z}}{(\hat{h}+\sin\hat{z})^3}, \tag{45}$$

$$\hat{p}_0 = \frac{1}{2(\hat{h}^2-1)}\left[\frac{\hat{A}_0 + \hat{h}(12-6\hat{V}_0)\cos\hat{z}}{(\hat{h}+\sin\hat{z})^2}\right] + \frac{\cos\hat{z}}{2(\hat{h}^2-1)^2}\frac{2(\hat{A}_0\hat{h}+12+6\hat{V}_0) + \hat{h}[(12+6\hat{V}_0)\hat{h}+\hat{A}_0]}{\hat{h}+\sin\hat{z}} + \frac{2\hat{h}(\hat{A}_0+12+6\hat{V}_0) + (12+6\hat{V}_0)\hat{h} + \hat{A}_0}{2(\hat{h}^2-1)^2}\int\frac{d\hat{z}}{\hat{h}+\sin\hat{z}} + \hat{P}_0. \tag{46}$$

Since we must consider both the upper and lower regions, we are left with five constants $\hat{V}_0$, $\hat{A}_{0u}$, $\hat{A}_{0l}$, $\hat{P}_{0u}$ and P_{0l}, to be obtained from dynamical considerations. Lowest-order force equilibrium of the sheet, cf. (5) and (6), yields

$$\mathscr{F}.\mathbf{e}_z = \frac{\mu c k}{\epsilon}\left\{\left\langle\left(\frac{\partial \hat{u}_0}{\partial \hat{y}} + \hat{p}_0 \cos \hat{z}\right)_{(\hat{z}_0, \hat{y}_0)}\right\rangle_u - \left\langle\left(\frac{\partial \hat{u}_0}{\partial \hat{y}} + \hat{p}_0 \cos \hat{z}\right)_{(\hat{z}_0, \hat{y}_0)}\right\rangle_l\right\} = 0, \quad (47)$$

$$\mathscr{F}.\mathbf{e}_y = \mu c k\{-\langle \hat{p}_0\rangle_u + \langle \hat{p}_0\rangle_l\} = 0. \quad (48)$$

Application of the momentum theorem to the fluid, cf. (8), yields, to lowest order,

$$\left\langle\left(\frac{\partial \hat{u}_0}{\partial \hat{y}} + \hat{p}_0 \cos \hat{z}\right)_{(\hat{z}_0, \hat{y}_0)}\right\rangle_u - \left\langle\left(\frac{\partial \hat{u}_0}{\partial \hat{y}}\right)_{\hat{y}=\hat{h}_1}\right\rangle_u = 0, \quad (49)$$

$$-\left\langle\left(\frac{\partial \hat{u}_0}{\partial \hat{y}} + \hat{p}_0 \cos \hat{z}\right)_{(\hat{z}_0, \hat{y}_0)}\right\rangle_l + \left\langle\left(\frac{\partial \hat{u}_0}{\partial \hat{y}}\right)_{\hat{y}=-\hat{h}_2}\right\rangle_l = 0. \quad (50)$$

Equations (47), (49) and (50) determine $\hat{V}_0$, $\hat{A}_{0u}$ and $\hat{A}_{0l}$; thence, from (41) and (48), $\hat{P}_{0u} = \hat{P}_{0l} = 0$. Notably, the coefficient of the third term in (46) vanishes, so that $\hat{p}_0$ is a simply periodic function of z (though no longer proportional to $\hat{v}(\hat{z}_0, \hat{y}_0)$ as in the biharmonic case). We obtain

$$\hat{V}_0 = 3\frac{(\hat{h}_2^2-1)^{\frac{1}{2}}(2\hat{h}_2^2+1)+(\hat{h}_1^2-1)^{\frac{1}{2}}(2\hat{h}_1^2+1)}{(2\hat{h}_2^2+1)(\hat{h}_1^2-1)^{\frac{1}{2}}(\hat{h}_1^2+2)+(2\hat{h}_1^2+1)(\hat{h}_2^2-1)^{\frac{1}{2}}(\hat{h}_2^2+2)}, \quad (51)$$

$$\hat{A}_{0u} = \frac{-18\hat{h}_1(2\hat{h}_2^2+1)[(\hat{h}_1^2-1)^{\frac{1}{2}}+(\hat{h}_2^2-1)^{\frac{1}{2}}]}{(2\hat{h}_2^2+1)(\hat{h}_1^2-1)^{\frac{1}{2}}(\hat{h}_1^2+2)+(2\hat{h}_1^2+1)(\hat{h}_2^2-1)^{\frac{1}{2}}(\hat{h}_2^2+2)} \quad (52)$$

and an analogous expression for $\hat{A}_{0l}$. The average rate of working is, to lowest order,

$$E = \left(\frac{\mu c^2 k}{\epsilon}\right) \times 6\left(\frac{1}{(\hat{h}_1^2+2)(\hat{h}_1^2-1)^{\frac{1}{2}}} + \frac{1}{(\hat{h}_2^2+2)(\hat{h}_2^2-1)^{\frac{1}{2}}}\right). \quad (53)$$

If $h_1 \neq h_2$, it can be shown that a net torque will be exerted on the sheet, tending to turn it away from the near wall. This torque vanishes when $h_1 = h_2$; thus, the centre of the channel is the 'preferred' position, just as in the biharmonic case. Thence, in dimensional variables,

$$\frac{V_0}{c} = \frac{3}{(h/b)^2+2}. \quad (54)$$

Equations (51) or (54) clearly indicate that to lowest order the velocity of propulsion is bounded by the wave speed. This contradicts Reynolds' conclusion $\epsilon^2 V_2 \lesssim 3c$, a result obtained, however, in the improper limit $\epsilon \to kh \to 0$ of the biharmonic analysis. By analogy with the results for an isolated sheet, we might expect that the next-lowest-order correction to V is negative, cf. Taylor and Blake.

It is noteworthy here that, since $b = O(h)$, the longitudinal components of the sheet surface oscillations do not influence V to lowest order, a result different from that in the biharmonic case, cf. (28). The sheet here is effectively sinusoidal. Clearly the biharmonic limit $kh \to 0$, $b \ll h$ should coincide with the lubrication-

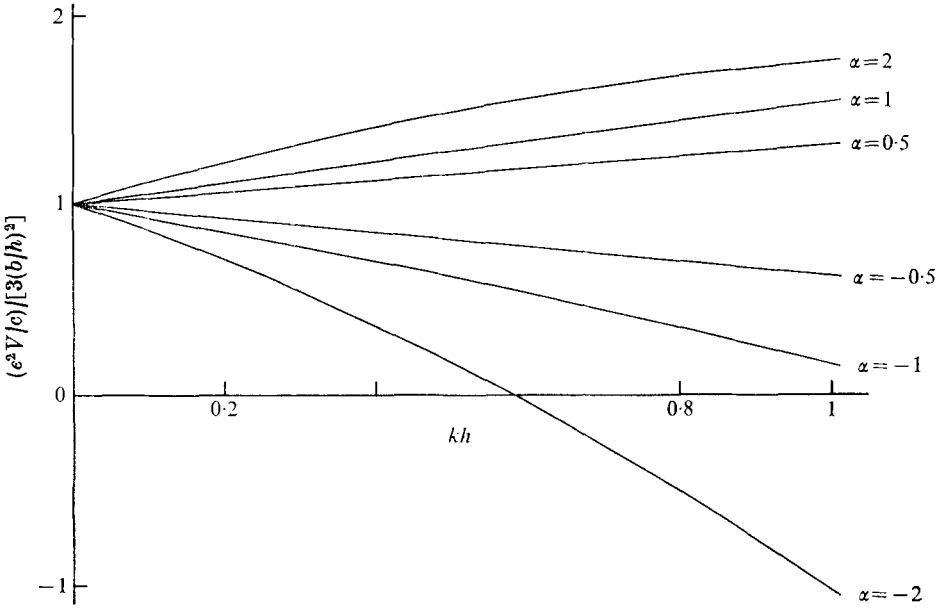

FIGURE 3. Convergence of the biharmonic propulsive velocity to the limiting lubrication-theory result. In this limit we fix $b/h \ll 1$ and let $h \to 0$ for fixed k.

theory limit $b/h \to 0$. Indeed, for a sheet at the centre of a channel, we have from (28), (29), (51) and (53), fixing k,

$$\lim_{b/h\to 0}\left(\frac{V_0}{c}\right)_L = \lim_{\substack{kh\to 0\\ b\ll h}}\left(\frac{\epsilon^2 V_2}{c}\right)_B = 3\left(\frac{b}{h}\right)^2, \tag{55a}$$

$$\lim_{b/h\to 0}\left(\frac{E}{2\mu c^2 k}\right)_L = \lim_{\substack{kh\to 0\\ b\ll h}}\left(\frac{E}{2\mu c^2 k}\right)_B = 6\left(\frac{b}{h}\right)^2\frac{1}{(kh)}, \tag{55b}$$

where the subscripts L and B denote lubrication-theory and biharmonic results respectively. The transition from the biharmonic behaviour, which is strongly dependent upon a and d, to the lubrication-theory result is best seen by noting that as $kh \to 0$

$$\left[\left(\frac{\epsilon^2 V_2}{c}\right)\frac{1}{3(b/h)^2}\right]_B \cong 1+\tfrac{2}{3}(kh)\left(\frac{a}{b}\right)-(kh)^2\left[\left(\frac{a}{b}\right)^2+\left(\frac{d}{b}\right)^2\right], \tag{56a}$$

$$\left[\frac{E}{(2\mu c^2 k)}\frac{kh}{6(b/h)^2}\right] \cong 1+(kh)\left(\frac{a}{b}\right)+\tfrac{1}{3}(kh)^2\left[\left(\frac{a}{b}\right)^2+\left(\frac{d}{b}\right)^2\right]. \tag{56b}$$

Figure 3 illustrates the transition for propulsive velocity.

4. Combined biharmonic–lubrication-theory problem

Let us now consider the case $h_1 k \ll 1$, $h_2 k \geqslant O(1)$. Here the swimming sheet is very close to the upper wall only. We may therefore expect lubrication theory to be applicable in the upper region, and a biharmonic analysis to be appropriate

in the lower one. The assumption $\epsilon \ll 1$ provides the bridge between the two approaches. From the lubrication-theory analysis we note that the dimensional average streamwise force per wavelength acting on the upper sheet surface is

$$(\mathscr{F}.\mathbf{e}_z)_u = \frac{\mu c k}{\epsilon}\left\langle\left(\frac{\partial \hat{u}_0}{\partial \hat{y}} + \hat{p}_0 \cos \hat{z}\right)_{(\hat{z}_0, \hat{y}_0)}\right\rangle_u + \ldots . \tag{57}$$

The biharmonic analysis in the lower region yields

$$(\mathscr{F}.\mathbf{e}_z)_l = -\mu c k\left\langle\left(\frac{\partial \tilde{u}_0}{\partial \tilde{y}} + \frac{\partial \tilde{v}_0}{\partial \tilde{z}}\right)_{\tilde{y}=0}\right\rangle_l + \ldots . \tag{58}$$

Owing to the thin upper region, propulsion is of 'zero order' in ϵ, and the first term in (57) will not vanish. However, the force on the lower sheet surface is one order of magnitude smaller than that on the upper surface. Hence the lowest-order force equilibrium for the sheet yields

$$\langle(\partial \hat{u}_0/\partial \hat{y} + \hat{p}_0 \cos \hat{z})_{(\hat{z}_0, \hat{y}_0)}\rangle_u = 0. \tag{59}$$

Using the expressions for $\hat{u}_0$ and $\hat{p}_0$, cf. (42) and (46), in (62) and the momentum theorem for the upper region, cf. (8), we obtain

$$\frac{V_0}{c} = \frac{3}{(h_1/b)^2 + 2}. \tag{60}$$

Note that (60) is identical with the lubrication-theory result for $h_1 = h_2$, cf. (54). That is, when one wall is removed to infinity, propulsive velocity is obtained from the solution for the region between the sheet and the near wall, regardless of the distance to that wall.

When transverse force equilibrium, moment equilibrium and the rate of working of the sheet are considered, again only the lubrication-theory region contributes to lowest order. Thus

$$E = \left(\frac{\mu c^2 k}{\epsilon}\right)\frac{6}{(\hat{h}_1^2 + 2)(\hat{h}_1^2 - 1)^{\frac{1}{2}}}. \tag{61}$$

It is readily shown that the lowest-order transverse force equilibrium of the sheet is satisfied provided that $\hat{P}_{0u} = 0$. However, a torque once again appears, tending to rotate the entire sheet away from the near wall. This is in contrast to the entirely biharmonic problem with $\hat{h}_2 \to -\infty$, where no such torque appears. It is therefore suggested that, when the sheet is placed relatively close to a single wall, it will tend to be rotated away from the wall; but when sufficiently distant from the wall (and, of course, parallel to it) the sheet will continue to swim parallel to the wall. When placed between the two walls of a channel of finite width, the sheet will tend to swim along the centre of the channel. Finally, there exists the same coincidence of biharmonic and lubrication-theory limits here as was demonstrated in §3 for a sheet in a channel.

5. Practical considerations

The analyses in §§2–4 indicate that, when a wavy sheet is in proximity to a flat wall or walls, both the propulsive velocity and rate of working can be significantly higher than when the sheet is isolated. It would seem unlikely that most

micro-organisms could sustain their propagated wave forms when faced with, say, a tenfold increase in energy output, as can occur here. More likely the beat would be altered. It is, therefore, appropriate to consider propulsive velocity at a fixed rate of working, allowing the propagated wave speed c and wave shape to vary with separation distance from the wall. We shall consider a swimming sheet either near a single wall, or at the centre of a channel of finite width. The rate of working shall remain fixed at its value for a sheet in an infinite fluid. In allowing for variations in wave shape, a reasonable constraint is that an effective length of the infinite sheet remains constant. Since $bk \ll 1$, the length l of a finite sheet containing n wavelengths is

$$\begin{aligned} l &= (2\pi/k)\, n[1 + \tfrac{1}{4}(bk)^2 + O(bk)^4] \\ &= (2\pi/k_\infty)\, n_\infty[1 + \tfrac{1}{4}(b_\infty k_\infty)^2 + O(b_\infty k_\infty)^4], \end{aligned} \tag{62}$$

where the subscript ∞ refers to an isolated sheet. Note that, to $O(bk)^2$, l is independent of the values of a and d. The pertinent rate of working is now nE, an effective total for the sheet. We shall take $d = 0$, it being readily shown that this value maximizes the modulus of the propulsive velocity subject to constant nE. In addition, we shall introduce two simplifications. First, we assume that the small amplitude restriction is strictly maintained, i.e. $bk = b_\infty k_\infty$. Second, we shall consider separately variations in wave shape and propagated wave speed.

Consider now $\Delta V \equiv V/(\epsilon^2 V_2)_\infty$ and $\Delta E \equiv nE/(nE)_\infty$, where V is the lowest-order component of the propulsive velocity, i.e. $\epsilon^2 V_2$ or V_0, for the biharmonic or lubrication-theory problems, respectively. In general, ΔV is a function of a, b, k, c, h, a_∞, b_∞, k_∞, and c_∞, ΔE a function of these parameters and, additionally, n and n_∞. From (62) and the requirement $bk = b_\infty k_\infty$, we have $n/n_\infty = k/k_\infty$. Our constraint on the rate of working becomes $\Delta E = 1$. These two conditions yield a unique relation among the wave parameters c/c_∞, k/k_∞, α, α_∞ and kh, where $\alpha \equiv a/b$. If we fix $k = k_\infty$ and $\alpha = \alpha_\infty$, we can then obtain c/c_∞ as a function of α and kh. That is, we can determine the change in propagated wave speed that satisfies the energy output constraint. We can subsequently obtain the change in propulsive velocity, viz. ΔV. If we wish to investigate changes in wave shape, we fix $c = c_\infty$ and $k = k_\infty$, determining α and thence ΔV as functions of kh and α_∞.

5.1. *Biharmonic analysis*

Using (28), (29) and (62), we define

$$\begin{aligned} \Delta V &\equiv \epsilon^2 V_2/(\epsilon^2 V_2)_\infty \\ &= \left(\frac{c}{c_\infty}\right)\left\{\frac{\sinh^2 kh + (kh)^2}{\sinh^2 kh - (kh)^2} - \alpha^2 + 2\alpha\left[\frac{\sinh kh \cosh kh - kh}{\sinh^2 kh - (kh)^2}\right]\right\}\frac{1}{1 + 2\alpha_\infty + \alpha_\infty^2}, \end{aligned} \tag{63}$$

$$\begin{aligned} \Delta E_C &\equiv nE_C/(nE)_\infty \\ &= \left(\frac{ck}{c_\infty k_\infty}\right)^2\left\{\frac{kh + \sinh kh \cosh kh + 2\alpha(kh)^2 + \alpha^2[\sinh kh \cosh kh - kh]}{\sinh^2 kh - (kh)^2}\right\}\frac{1}{1 + \alpha_\infty^2}, \end{aligned} \tag{64}$$

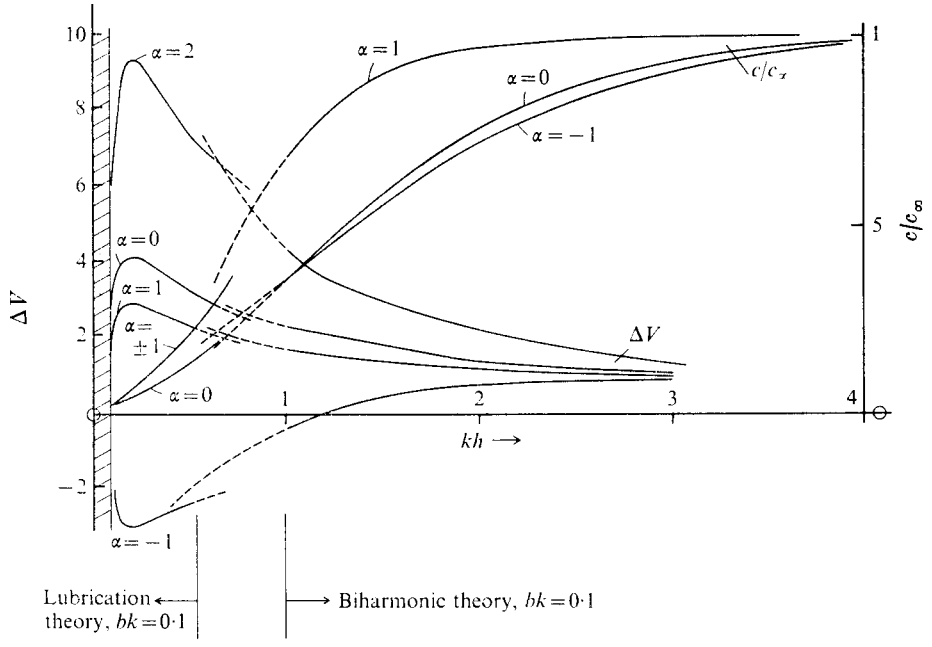

FIGURE 4. Lowest-order variation of $\Delta V = V/V_\infty$ and c/c_∞ with kh for a sheet in a channel, with the rate of working fixed at that for an isolated sheet. Here $b = b_\infty$, $k = k_\infty$ and $a = a_\infty$. The c/c_∞ curve for $\alpha = 2$ lies so close to the $\alpha = 0$ curve that it is omitted for the sake of clarity.

$$\Delta E_W \equiv nE_W/(nE)_\infty$$
$$= \left(\frac{ck}{c_\infty k_\infty}\right)^2 \left\{\frac{kh + \sinh kh \cosh kh + 2\alpha\,(kh)^2 + \alpha^2\,[\sinh kh \cosh kh - kh]}{\sinh^2 kh - (kh)^2} + 1 + \alpha^2\right\} \times \frac{1}{2(1+\alpha_\infty^2)}, \quad (65)$$

where the subscripts C and W refer to a sheet at the centre of a channel or near a single wall, respectively. For fixed wave size and shape, c/c_∞ is obtained from (64) or (65); thence (63) determines ΔV. Typical results for a sheet in a channel are shown in figure 4. It should be noted that, since $b \ll h$, both the denominator and numerator of ΔV and ΔE approach zero in the biharmonic limit $kh \to 0$. If the b dependence is removed by factoring, then ΔV and ΔE become singular as $1/(hk)^2$ and $1/(kh)^3$, respectively, indicating the inapplicability of this limit. Note also that, with decreasing kh, c/c_∞ decreases, while ΔV increases for $\alpha \geqslant 0$ but decreases when $\alpha > 0$. The corresponding behaviour for a sheet near a single wall is very similar, the values of $|\Delta V|$ and c/c_∞ being somewhat larger.

If variations in wave shape are of interest, then (64) or (65) is solved for α. Although these equations are quadratic in α, we choose that value of α which allows $\Delta V \to 1$ as $kh \to \infty$. For certain values of kh and α_∞, complex solutions for α are obtained, indicating that in those circumstances the fixed rate of working constraint is not obtainable. Typical results for a sheet near a single wall are shown in figure 5. Summarizing these results, for decreasing kh, ΔV increases

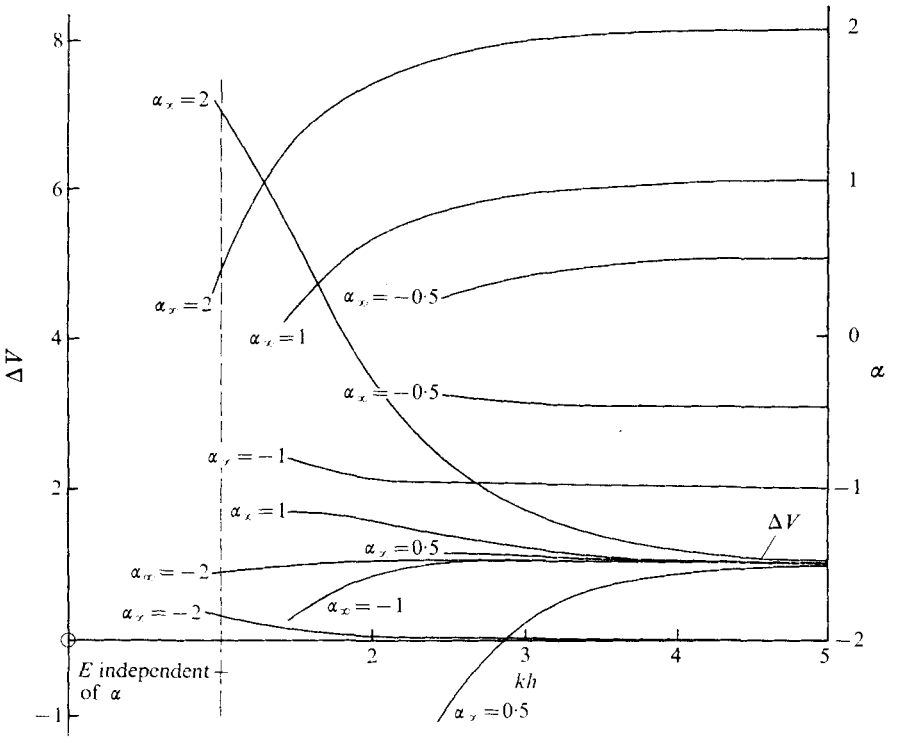

FIGURE 5. Lowest-order variation of ΔV and $\alpha = a/b$ with kh for a sheet near a single wall, with the rate of working fixed at that for an isolated sheet. Here $c = c_\infty$, $b = b_\infty$ and $k = k_\infty$, so that a varies. Curves not extending throughout $1 \lesssim kh \leqslant 5$ indicate that the energy constraint cannot be satisfied for all combinations of α_∞ and kh. In the lubrication-theory region, i.e. $kh \ll 1$, E is independent of α. Thus the constraint can never be satisfied and the analysis has no meaning there.

and α decreases for $\alpha_\infty > 0$; while ΔV decreases and α increases for $\alpha_\infty < 0$. For a sheet in a channel, the corresponding results are again very similar, the tendency being for slightly lower $|\alpha - \alpha_\infty|$ and $|\Delta V|$.

Finally, let us consider the special case of an effectively sinusoidal sheet, $\alpha = 0$, fixing $c = c_\infty$ and allowing $n/n_\infty = k/k_\infty = b_\infty/b$ to vary. The results, illustrated in figure 6, indicate that, as kh decreases, the sheet must reduce the effective number of wavelengths. Thus the waves become larger owing to simultaneous increases in both amplitude and wavelength; and the beat frequency kc decreases.

5.2. *Lubrication theory*

For a sheet swimming in a narrow channel or near a single wall such that $kh \ll 1$, we have, using (53), (54), (60), (61), and (62),

$$\Delta V = \left(\frac{c}{c_\infty}\right) \frac{6}{(kh)^2 + 2(bk)^2} \left(\frac{1}{1 + 2\alpha - \alpha^2}\right), \tag{66}$$

$$\Delta E = \left(\frac{ck}{c_\infty k_\infty}\right)^2 \frac{6}{[(kh)^2 + 2(bk)^2][(kh)^2 - (bk)^2]^{\frac{1}{2}}} \left(\frac{1}{1 + \alpha^2}\right). \tag{67}$$

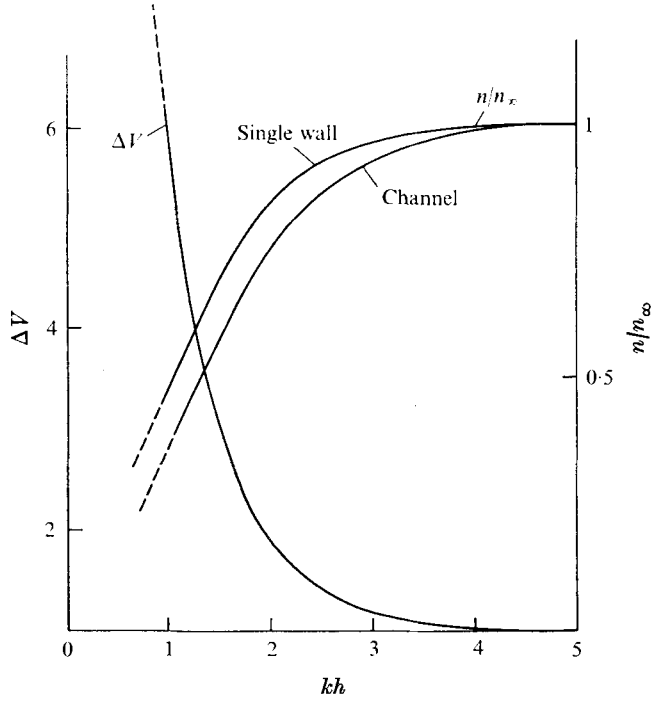

FIGURE 6. Lowest-order variation of ΔV and n/n_∞ with kh for a sheet with the rate of working fixed at that for an isolated sheet. Here $c = c_\infty, bk = b_\infty k_\infty$ and we have considered a sinusoidal sheet, viz. $\alpha = 0$.

Allowing variations in wave speed alone to satisfy $\Delta E = 1$, c/c_∞ and ΔV are determined from (67) and (66), respectively, cf. figure 4. In figure 4, note the good agreement between the acceptable biharmonic limit $kh \sim 1$ and the lubrication-theory results. Note also that ΔV passes through an extremum as kh decreases. Indeed, it is readily shown that the extremal value is

$$\Delta V = [3^{\frac{1}{2}}/(bk)^{\frac{1}{2}}]\left[\frac{1+\alpha^2}{1+2\alpha-\alpha^2}\right],$$

with $h = 2b$ and $c/c_\infty = (3^{\frac{1}{2}})(bk)^{\frac{3}{2}}(1+\alpha^2)$. Thus, if $1-2^{\frac{1}{2}} < \alpha < 1+2^{\frac{1}{2}}$, this extremum is a maximum, cf. figure 7. Since V and E are independent of α in the lubrication-theory analysis, no optimization with respect to α is possible, cf. figure 5. However, if only the wave size is allowed to vary subject to $\Delta E = 1$, $bk = b_\infty k_\infty$, and constant effective length, cf. (62), we again determine that, with decreasing kh, ΔV increases as the effective number of wavelengths decreases.

6. Discussion

This paper is a simple study of whether or not a motile micro-organism can derive propulsive advantage from its proximity to a solid boundary or boundaries. The results of §5 suggest that such an advantage is indeed possible. An obvious

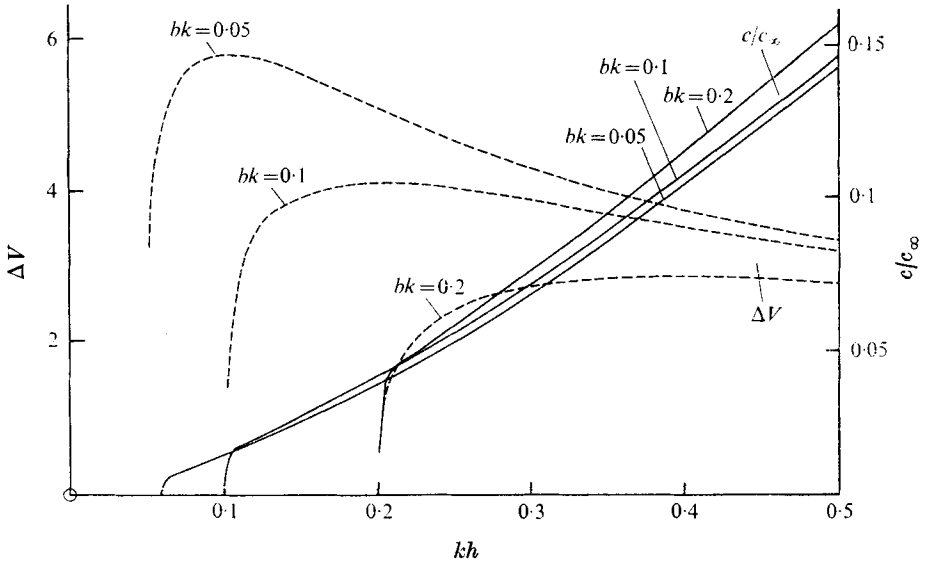

FIGURE 7. The presence of a ΔV maximum, at optimal spacing $h = 2b$, for a sheet either in a channel or near a single wall. Here $b = b_\infty$, $k = k_\infty$ and the rate of working is fixed at that for an isolated sheet. These examples are for $\alpha = 0$.

means of achieving this is a reduction in propagated wave speed, and thus beat frequency. For such a reduction, there exists an optimal separation distance of twice the wave amplitude. This spacing is optimal in that for certain wave shapes ΔV is a maximum, though for other shapes it is a minimum. Likewise, changes in wave shape alone can abet or diminish propulsive velocity subject to a fixed rate of working. In general, a small number of large waves is preferable to a large number of small waves, this condition being dependent, of course, upon the fact that pitching motions are neglected.

The effect of the wall becomes significant when $kh \lesssim 5$, i.e. the separation distance decreases below the order of a wavelength. For $kh \gtrsim 1$, the propulsive velocity and rate of working are sensitive to changes in wave shape, transverse oscillations becoming relatively more important than longitudinal ones as kh decreases. Indeed, with decreasing kh, reversals in the direction of propulsion occur for certain shapes.

It should be emphasized that this simple two-dimensional model simulates a micro-organism swimming parallel to a wall and beating in a plane perpendicular to that wall. This is a very special case, since among those micro-organisms that propagate reasonably uniform planar waves, e.g. some sea-urchin spermatozoa, many tend to roll owing to asymmetries in the head. It is often observed that, when flagellated micro-organisms such as spermatozoa are confined to swim in a thin lamina of fluid between a microscope slide and coverslip, their beat appears to be confined to a plane parallel to the walls, not perpendicular to them. Therefore,we must again caution that the applicability of these results is qualitative at best. Preliminary studies of wall effects on the propulsion of flagel-

lates of finite length and width do suggest that increases in both propulsive velocity and rate of working occur (Lighthill 1974; Katz & Blake 1974). The tendency to be turned away from a wall has been demonstrated both theoretically and experimentally for sedimenting rods by de Mestre (1973) and de Mestre & Russel (1974). The author is presently engaged in obtaining cinemicrographic data with which to compare these results.

In the context of spermatozoan transport within the male and female reproductive tracts, it is indeed true that the spermatozoa may at times be in close proximity to other solid, and possibly moving objects. Biharmonic analyses for wavy sheet models of such situations have been obtained, cf. Katz (1972) and Smeltzer (1972), and the author is presently completing the lubrication-theory analysis for several pertinent problems. However, it must be remembered that the scale of much of the activity of the male and female tracts is considerably larger than that of the spermatozoa themselves. Therefore, while mathematical extension of these methods to motile walls seems both attractive and tractable, obvious geometrical factors severely limit the applicability of the results.

Comments from Prof. S. A. Berger and Prof. Sir James Lighthill are very much appreciated. The author gratefully acknowledges the support of a Population Council Postdoctoral Fellowship.

REFERENCES

BLAKE, J. R. 1971 Infinite models for ciliary propulsion. *J. Fluid Mech.* **49**, 209–222.

KATZ, D. F. 1972 On the biophysics of *in vivo* sperm transport. Ph.D. thesis, University of California, Berkeley.

KATZ, D. F. & BLAKE, J. R. 1974 Flagellar motions near walls. (In preparation.)

LIGHTHILL, M. J. 1974 Mathematical biofluiddynamics. (In the Press.)

MESTRE, N. J. DE 1973 Low Reynolds number fall of slender cylinders near boundaries. *J. Fluid Mech.* **58**, 641–656.

MESTRE, N. J. DE & RUSSEL, W. B. 1974 Slender cylinder near a plane wall in Stokes flow. (Submitted to *J. Engng Math.*)

REYNOLDS, A. J. 1965 The swimming of minute organisms. *J. Fluid Mech.* **23**, 241–260.

SMELTZER, R. T. 1972 A low Reynolds number flow problem with application to spermatozoan transport in cervical mucus. M.S. thesis, Massachusetts Institute of Technology.

TAYLOR, G. I. 1951 Analysis of the swimming of microscopic organisms. *Proc. Roy. Soc.* A **209**, 447–461.